 DOI: 10.1002/masy.201200119

From Heterocoagulation to Biorecognition: Preparation of Surfaces for Direct Measurement of Their Interactions in a Surface Force Apparatus

Patrick Kékicheff

Summary: Due to the atomic resolution in surface separation accessible the Surface Force Apparatus technique provides an avenue for investigating the interactions in real systems, provided the model surfaces chosen for study have both equivalent intricate surface chemistry and structural properties. To overcome the difficulty of surface-altering treatments when preparing suitable surfaces for the SFA and to realize interfaces fully representative of real systems immersed in solvents we have developed different experimental procedures. In particular, adsorption of nanoparticles from bulk colloidal dispersions, controlled solvent flow for coating substrates with polyelectrolytes multilayers, Langmuir Blodgett deposition of phospholipids membranes inserting ligands/receptors, all illustrate how one can get insights into subtle phenomena revealed by the force-distance profiles when the true colloidal state is maintained, biomaterials are built and molecular recognition is involved.

Keywords: biomaterials; coatings; colloids; molecular recognition; polyelectrolytes

Introduction

Surface forces play a crucial role in the stabilisation of colloidal suspensions, aggregation, phase behaviour in surfactant systems, membrane behaviour, recognition between protein and biological species, adhesion, lubrication, coating, and many other applied and commercially important areas (detergency, food industry, cosmetics, drug delivery, enhanced oil recovery, biocompatibility, etc.).[1] Both repulsive and attractive forces can occur between surfaces, and they can extend in range from only a few molecular diameters to micrometers. The materials constituting the bodies may be crystalline, amorphous, metallic, and the interfaces may be solid or liquid, while the space between the bodies may consist of pure liquids or solutions, gases or vapors, or even vacuum in certain industrial processes.

Institut Charles Sadron, C.N.R.S., Université de Strasbourg, 23, rue du Loess, B.P. 84047, 67034-Strasbourg cedex 2, France
E-mail: patrick.kekicheff@ics-cnrs.unistra.fr

The surface properties of the bodies are usually modified by the adsorption of various molecular species, e.g. vapor, liquid condensates (as bridges of capillary-condensed liquid), ions, surface active agents and macromolecules. Nature and industrial processes take advantage of these surface properties modifications as the effects on the surface forces allow similar and dissimilar materials to arrange themselves into intricate structures and to form complex composite architectures, as found in many fields spanning from the phenomena of heterocoagulation in colloid science to biorecognition between ligands and receptors attached to surfaces. Therefore the subtle interplay between all the interactions acting between two bodies must be understood not only between like materials, but also between *unlike* materials; its control will allow the scientists and engineers to develop new advanced materials.

Surface forces have been inferred from different techniques, which can be classified into two complementary categories.[2] Either the interaction profile is measured at

constant chemical potential of all species (such as in force balance and spring devices), or the response to a change of the chemical potential of solvent for example is investigated (such as in osmotic equilibria based methods and as in light, X-rays or neutrons scattering experiments). Concerning the first category of investigation at constant chemical potential, the techniques use two macroscopic surfaces of the same nature as the particle surfaces, and the force-to-distance relation is measured with a deflection method (surface force balances,[3,4] surface force apparatus,[5,6] atomic force microscope,[7] etc.). The main difficulty is to make such surfaces or to stick the microscopic particles, without altering the surface chemistry of their interfaces, to the macroscopic surfaces of these devices.

By means of the atomic force microscope (AFM) technique, the task is difficult as the size of the AFM cantilever is extremely small; nevertheless some advances have been noted in the literature.[8,9] Although having become less popular in the recent years, the Surface Force Apparatus (SFA)[6] technique presents several advantages. Due to the atomic resolution in surface separation accessible, the SFA technique allows a direct measurement of the interaction between two macroscopic surfaces (of cm^2 area) immersed in a solution. The technique has been widely used for the last 30 years to investigate interactions between surfaces of different nature immersed in aqueous or organic solutions.[1] In most of the cases the studies have reported the force – distance profile acting between two opposite *like* surfaces, that is opposite surfaces whose interfaces have the same physico-chemical properties and the same structure (in terms of spatial organization or of roughness). But even in the case of interactions between like surfaces it was already noted that dramatic effects may arise when the configuration departs from a strict symmetry: for illustration, the adhesion between two mica crystal surfaces is effected by the rotational mismatch of surface lattices brought to contact,[10] a repulsive interaction may turn to attractive when the order parameter is effected by the roughness of one of the surface.[11]

Despite some significant progress,[1,2] so far the connection of those SFA measurements to any real system in colloidal science, in biology, etc., has been remote. The paucity of the reported data is due to the difficulties encountered in mimicking a real interface. This is because the model surfaces chosen for study have been much simpler than the actual colloid or membrane/aqueous solution interfaces. Attempts to relate the measured force with colloidal stability or biological recognition can be only of limited success as the intricate surface chemistry is not equivalent. However, some insights have been gained thanks to the direct investigation of the force-distance relationships between phospholipids membranes,[12–15] or among biomolecules:[16] for example the behavior of adsorbed polypeptides and proteins on macroscopic substrates,[17–21] the key-lock interaction between streptavidin and biotin,[22,23] the specific interaction between nucleotides,[24] the complex binding mechanism in cadherin adhesion,[25,26] the tethered ligand-receptor bond formation[27,28] have been directly measured by means of the SFA technique. The comparison is nevertheless rendered difficult when the intrinsic fluctuations of the actual interfaces are restricted due to the rigid coated-surfaces of the SFA device[29] (this problem can be overcome as we showed for freely suspended membranes[30,31]). The most commonly used substrate has been muscovite mica — an aluminosilicate mineral, which can be cleaved along a basal plane to produce the large, 1–3 μm thick, atomically smooth and optically transparent sheets required for the experiment. The core problem is thus to promote adequate macroscopic surfaces to be used for direct force measurements. This being realized will allow direct comparison with colloidal stability or biological recognition for instance.

The work presented in this and subsequent articles deals further with these issues. The question addressed in this report is the following. How can one prepare macroscopic

surfaces of the SFA to accurately mimic a real interface such as an oxide/aqueous solution interface, a biocompatible interface, or a lipid membrane containing ligands in order to study the biological recognition with a receptor? In this report the focus is more on the methodology of the surface preparation rather than on the interpretation of the measured force-distance profile. As one will see, our methods of preparing the macroscopic surfaces used in the SFA can be shown to be easily generalized to any real system, as the native surface chemistry of the interface is maintained. We present three main categories of surface preparation: adsorption of nanoparticles from bulk solution, polyelectrolyte coating through a controlled solvent flow, Langmuir-Blodgett deposition. In the three cases, the experiments, performed entirely within the liquid chamber of the SFA, prevent the interface (oxide, polyelectrolyte, membrane) from experiencing any environment outside of its native aqueous state. This preserves the reactive sites which would otherwise collapse in the usual drying and washing processes. As every SFA surface can be prepared independently, not only symmetric configurations of two like interacting surfaces can be realized, but more interestingly asymmetric configurations can be realized in a controlled way to directly measure the interactions between two unlike surfaces. The play with different surface configurations allows us to investigate the mechanical stability of thin films, the colloidal stability of nanoparticles dispersions, the heterocoagulation occurring between charged surfaces, the origin of adhesion at contact, the ligand-receptor specific interaction, etc.

Experimental Part

Materials

All solutions were freshly prepared and filtered (0.22 μm) before use. Ultra pure water was obtained from a commercial Millipore purification system (MilliQ Gradient system). The end product had a conductivity of 18.2 MΩ cm^{-1}, showed no bubble persistence, and had a pH about 5.7 due to equilibration with dissolved atmospheric CO_2. As a precaution against dissolved silicate and other contamination, water drawn through the MilliQ unit was stored in a laminar flow cabinet in a stopped flask for no longer than 24 hours. Water was degased for 30 min under vacuum beforehand to reduce the possibility of small bubbles being trapped in the buildup of the thin films coating the macroscopic surfaces or being introduced into the chambers of the AFM and the SFA, and thus to avoid bubble formation between the surfaces.

Electrolytes were all analytical grade reagents obtained from Aldrich, BDH and Ajax Chemical Suppliers. These salts were used without further purification. Adjustment of the pH to a desired value was done by addition of small amounts of concentrated nitric acid or sodium hydroxide (both reagents were BDH Analar grade and were used as supplied). The MES-tris buffer solution at pH 7.4 consists of 100 mM/L $NaNO_3$ (Sigma, purity >99.99%), 25 mM/L 2-(*N*-morpholino)ethanesulfonic acid (MES) (Sigma, purity >99.5%), and 25 mM/L Tris(hydroxymethyl)aminomethane (Tris) (Sigma, purity >99.9%).

Silica sols were obtained from Eka Chemicals, Akzo Nobel (Bohus, Sweden) as aqueous dispersions of 30 percent by weight spherical, amorphous, non-porous silica particles of 14 nm diameter, supplied in electrolyte solutions (the specific surface area reported by EKA-NOBEL is 220 m^2/g, hence the commercial name of the sol: Bindzil 30/220). Stability against coagulation was imbued by the presence of sodium hydroxyde, which gave rise to the dispersions having pH of 10.2 at 20 °C. Dilute sols (volume fraction < 0.12) were prepared by diluting the concentrated sol with electrolyte solutions. Solutions were prepared gravimetrically.

The cationic poly(allylamine) PAH (CAS: 71550-12-4, $M_W = 70000$) and the anionic poly(styrene sulfonate) PSS (CAS: 25704-18-1, $M_W = 70000$) both from Sigma, were dissolved at 0.1 mg/mL in filtered

MES-Tris buffer solution. As the pH of 7.4 is kept constant, the polyelectrolytes remain ionized; this caution prevents collapse or swelling changes in the initial film structure that would otherwise be due to charge variations upon the subsequent deposition of additional layers.[32]

The phospholipids DSPE (1,2-Distearoyl-sn-glycero-3-phosphoethanolamine) and DPPC (1,2-dipalmitoyl-sn-glycero-3-phosphocholine), the chloroform (stabilized with ethanol) and the methanol were purchased from Sigma-Aldrich. Solutions of DSPE in chloroform/methanol/water 65:35:8 and DPPC in chloroform are used to spread the compounds on the free water surface of a Langmuir trough for Blodgett deposition of monolayer and bilayer on mica (see § 3-3).

Sliding Tethered Ligands (STLs) with a polyethylene glycol tether (PEG, $<N> = 222$) threaded through the cavity of a cholesteryl α-cyclodextrin (cholesteryl α-CD) and end-capped with adamantane at both chain ends, were synthesized by LIONS laboratory (Saclay, France) within the framework of a common research program funded by the ANR (Agence Nationale pour la Recherche, France). All details on the synthesis and on the characterization of the materials (by Infra Red Absorption Reflection Spectroscopy, Brewster Angle Microscopy, Atomic Force Microscopy, Neutron scattering techniques) were reported previously[33,34] or will appear shortly in forthcoming articles. Since adamantane forms a host-guest complex with β-CD, was also synthesized a cholesteryl β-cylodextrin (cholesteryl β-CD), as the receptor. The STLs or the cholesteryl β-CDs are inserted into the phospholipid bilayers deposited on mica by Langmuir-Blodgett technique by mixing these compounds with the DPPCs (see § 3-3).

Methods

Force Measurements Procedures

Force-distance profiles were measured using a home-made device based on the initial version of the Tabor-Israelachvili Surface Force Apparatus.[6] The new version of the apparatus allows enhanced spatial and time resolution and automation, as described in detail elsewhere.[35] The instrument allows the force F between two mica surfaces (of mean radius of curvature R) to be measured to within 50 nN as a function of the determined surface separation D, which can be measured to a typical accuracy of 0.2 nm, using multiple beam interferometry.[36] Normalized force F/R are uncertain to about 10%, as the error in the absolute scale is mainly dictated by the accuracy in the determination of R (≈2 cm). The smallest normalized force can be detected to within 0.003 mN/m, while the maximum reliably measurable force will depend on the mechanical compressibility of the entire system. Typically surface deformations occur for applied loads larger than 8 - 15 mN/m and F/R becomes meaningless due to the deformation of the glue beneath the mica sheet; for that reason, data are only reported for smaller loads, where the measured values of F/R correspond to the free energy E per unit area of two equivalent flat surfaces as given by the Derjaguin approximation ($F/R = 2\pi E$).[37]

After the assembly of the apparatus and measurement of the contact position in an atmosphere of dry nitrogen, the mica surfaces (glued down onto curved silica disks of radius ≈2 cm) were transferred into a sealed chamber or a Langmuir trough to add the assembly of the film coating the mica surfaces (see next section for the procedures). Once the coated-mica film was achieved the surfaces were repositioned into the SFA chamber. The operation was carried out under water in order to prevent any drying of the surfaces and all the coated-mica films were studied and kept in aqueous environment at all times to preserve their native structural organization.

The operation of removing and repositioning the silica disks with the coated mica back into the SFA yields an uncertainty of about 1 nm in the determination of the absolute separation. All operations were carried out in a laminar flow cabinet

(class 100) installed in a clean room (class 10000).

All SFA experiments were performed at $25.000 \pm 0.004\,^{\circ}C$. Such a thermal stability in the device allows the surfaces drift to be minimized.[35] After equilibration, the force *vs*. surface separation was measured, provided the thermal drift of the surfaces was negligible (< 1 nm per minute). The contact position was changed several times for each configuration of the surfaces in order to increase the reliability of the results. In particular, the adhesion values are only reliably determined if pristine contact positions are used as the local structure of the thin film coating the mica substrate may be altered from measurement to measurement if one single position is used. Indeed many situations may arise and have already been clearly identified by our previous investigations in several systems. Adsorbed particles may deform or be displaced (rolling laterally along the substrate, being pushed aside, or being desorbed) under applied loads.[19,21,38–40] Similarly contact of one coated-mica surface with another opposite surface (bare or coated substrate) may deform fragile supported objects such as phospholipids membranes or polyelectrolyte multilayers: elastic and even plastic irreversible deformation may be observed as the signature of interpenetration of the multilayers under compression.[41,42] Finally transfer of material from one surface onto the opposite one may occur depending on the strength of the mutual adhesion energy between particles or adjacent films compared to the adhesion energy between the adsorbed particles or the film with the substrate.[16,19,26,39,40] In such a case when the two adjacent layers adhere more strongly to each other than they adhere to the walls, patchy surfaces will be formed after separation: each surface will end up as being comprised of void domains where parts of the initial adsorbed layer have been transferred to the other surface, and of thick domains conversely made with two juxtaposed adsorbed layers parts. As a result the contact area will be extensively destroyed.

AFM Imaging

Images of the coated film surface onto the mica sheets were obtained with a Nanoscope IV (Digital Instruments, Inc., Santa Barbara, CA.) using microfabricated silicon AFM tips (cantilevers with a spring constant of 0.01 N/m) in the tapping mode in a liquid cell. The coated mica surfaces to be imaged were prepared following the procedure described above and monitored over time. Similar surface features were noted for images acquired over any scan size indicating that the thin coated film keeps its structural organization and physicochemical surface properties once built by our procedures. In particular no desorption of nanoparticles from the mica substrate, no significant structural rearrangement or diffusion of polyelectrolyte chains in and out of the entire PAH/PSS multilayered film, no distribution rearrangement of the anchored cholesteryl cyclodextrins and STL molecules inserted in the phospholipid membranes have been noted with time.

The mica surfaces used after completion of the SFA measurements were also observed under water in the tapping mode. To image these thin mica sheets that were first glued down onto the silica hemicylinders (radius of curvature ≈ 2 cm) of the SFA, the silica disks were dismounted from their SFA holders and mounted back into a homemade holder specially designed to fit the commercial AFM liquid cell. All operations were carried out under water in a laminar flow cabinet (class 100) installed in a clean room (class 10000). Comparison between the two sets of coated-mica surfaces indicate similar surface features for the same solution conditions. This observation indicates that the surface force measurements did not modify the surface coverage (no induced desorption of the inserted molecules and adsorbed nanoparticles in the coated films) and did not effect the structural and physicochemical properties of the thin coated film over period of days provided not too large loads were applied during force measurements.

Results and Discussion

Due to the atomic resolution in surface separation accessible, the Surface Force Apparatus allows the direct measurement of the interaction between two surfaces immersed in a solution. To mimic real systems the thin films which coat the mica sheets must fulfill two requirements when they are used as surfaces in a SFA device. First an homogeneously coated-mica film must be achieved as the force measured in the device is the result of all the interactions resulting from an area of about 50 μm in diameter. The second requirement concerns the achievement of a low surface roughness. This allows an entire force-distance profile down to contact to be measured allowing two main properties to be inferred: the long-range interaction and the adhesion at contact between layers.

Our methods of preparing the surfaces can be classified in three main categories illustrated in this report by three systems: (i) nanocolloids can be assembled in a monolayer by adsorption onto the substrate from bulk; (ii) a stack of polyelectrolyte multilayers can be deposited by successive solvent flow of alternate cationic and anionic polyelectrolytes; (iii) phospholipids membranes with inserted tethered ligand-receptor pairs with self-adjustable length can be deposited by Langmuir-Blodgett.

Using these procedures a macroscopic surface smooth at the nanometer or subnanometer scale is obtained only but which is fully representative of a colloidal particle-water interface or of a biological relevant interface. Thus the colloidal stability, the behavior of membranes, the ligand-receptor specific interaction, the development of biocompatible surfaces and of versatile bio-adhesive substrates, etc., can all be investigated. Our methods of preparing surfaces can be shown to be easily generalized to any real system. The advantages of all these three methods is here discussed in regard to the studied systems.

Coating Via Adsorption of Nanoparticles from Bulk Colloidal Solutions

In the procedure used, adsorption proceeds from a bulk dispersion of nanoparticles in which the substrate is immersed. As the probability of adhesion is governed by collision efficiency between the substrate (here an atomically smooth mica surface) and particles, solution conditions, such as pH, ionic strength, and volume fraction in particles must be determined in order to achieve an homogeneous and compact single layer of irreversibly adsorbed nanoparticles.

Optimum solution conditions result from the subtle interplay of the interactions between the particles with the mica and of the interactions between particles. Clearly a stable layer will be built on a macroscopic surface if mica attracts the particles.[43] However, a too long-range attraction will favor structures of low dimensionality (fractals) rather than compact layers.[44] The nature of the interaction between particles also governs the layer formation. When particles attract each other, clusters of aggregating particles occur in bulk yielding to a very rough interface of adsorbed inhomogeneous multilayers comprised with patches of aggregates protruding out. Conversely a too large repulsion between particles will lead to an incomplete layer due to the lateral repulsions between adsorbed particles.[45] Typically, as pointed out by Iler,[46] for small particles with specific areas of several hundred square meters per gram, sol concentrations of less than $\Phi = 0.005$ can be applied. The last requirement is that the adsorption energy should be relatively high (at least a few $k_B T$ per particle) in order to avoid a rapid desorption when the free particles are removed from the bulk.[47] The few comments above constitute the general frame of our approach.

After measurement of the contact position in an atmosphere of dry nitrogen to get the thickness of the mica sheets used in the SFA and the zero origin in separation, the adsorption of nanoparticles onto the mica surfaces can be obtained by two different

methods. In the first method[18,19,21,39,40] the mica surfaces are separated and *ca.* 40 cm^3 of ultra pure water (obtained with a Milli-Q plus (Millipore) system unit) is injected into the chamber with a syringe. Then the water is replaced with a dilute dispersion of colloids (volume fraction in particles of the order *ca.* $\Phi = 0.003$) and the surfaces are left separated a dozen of microns apart for about one hour. Finally the bulk colloidal dispersion is removed from the chamber and replaced by an aqueous electrolyte solution. The presence of minute traces of colloidal particles in the bulk is avoided by removing the solution from the chamber and replacing the discarded solution by the same fresh electrolyte solution several times. During every removal of bulk solution from the chamber special care is taken to leave a droplet of solution between the two surfaces in order to prevent any drying of the surfaces. This method yields a *symmetric* configuration where the two opposite surfaces in the SFA have adsorbed like colloidal particles and have built similar layer structure film.

In the second method each silica disk onto which is mounted the mica surface is transferred into a sealed chamber and immersed in a dilute dispersion of colloids for a certain duration of time (from a few minutes to several hours). Then the bulk colloidal dispersion is removed from the chamber and replaced several times by an aqueous electrolyte solution to remove any minute traces of non adsorbed or loose attached colloidal particles on the surface. As each mica surface is treated independently the procedure enables the adsorption equilibrium to be reached independently on each surface. Therefore *asymmetric* configurations can be realized in which one mica surface is coated with one type of colloids whereas the opposite one may be different: It may have a different surface coverage of like adsorbed particles, or it may be coated with another type of colloids, or even it may be a bare substrate without any coating (this latter situation is convenient to investigate the strength of adhesion between the particles and the substrate[39]). Once the coated-mica film is achieved the surfaces are repositioned into the SFA chamber. The operation is carried out under water in order to prevent any drying of the surfaces and all the coated-mica films are studied and kept in aqueous environment at all times to preserve their native structural organization.

Here we present results for colloidal silica obtained with the second method (reports on the use of the first method can be found in our previous SFA studies investigating proteins,[18,19,21] ceria[39] and silica nanoparticles[40]). Our illustration demonstrates that silica nanoparticles may adsorb directly onto mica surfaces, despite the fact that particles and substrates are both negatively charged in aqueous solutions above pH 2.[46,48] With this example we show that heterocoagulation can be directly investigated with direct force measurements by means of the SFA technique since we have succeeded in guarantying a true colloidal oxide-water interface.

The symmetric configuration of two similar silica-coated mica substrates is used to investigate the interaction between the silica adsorbed layers. As this report is illustrative of the experimental method that can be used for direct force measurements by means of the SFA technique we are presenting the results in the case of one solution condition only. The complete study with extensive variation of the solution conditions (pH, ionic strength, nature of the added salt) is beyond the scope of this article and will be reported elsewhere. Figure 1 shows typical images ($2 \times 2\,\mu m$; taken in tapping mode in the liquid cell of the AFM) of the adsorbed layer monitored with time in the presence of added potassium nitrate at 0.1 M and pH 9.

After a few hours the layer appears homogeneous over the whole substrate with an almost complete surface coverage by the adsorbed nanoparticles. Similar surface features were noted for images acquired over larger scan sizes. The particles appear as spots of 15–20 nm wide in a relatively smooth and flat film (the peak-to-

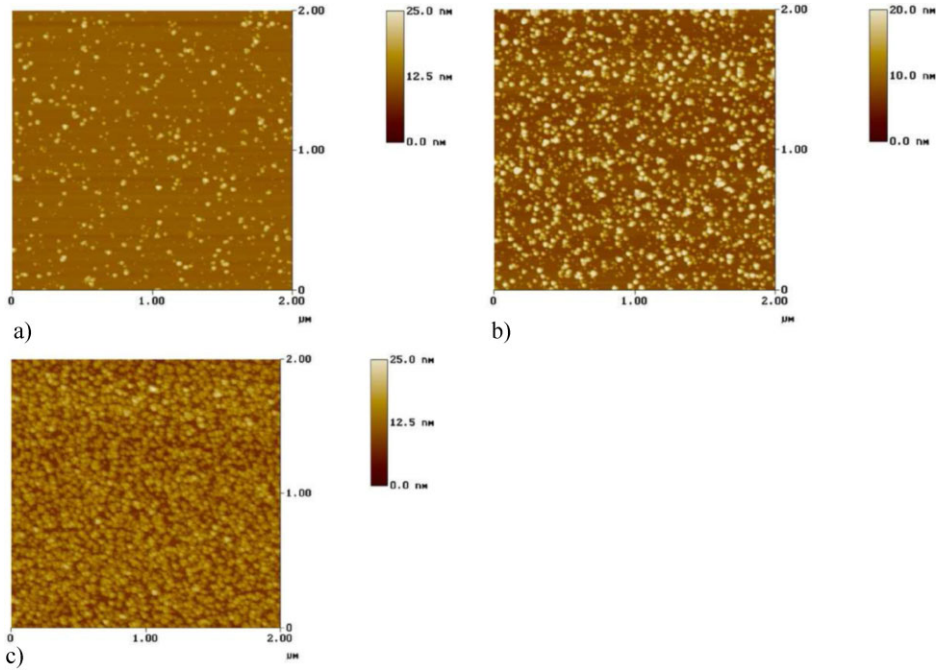

Figure 1.
Atomic Force Microscope in height tapping mode images ($2 \times 2\ \mu m^2$) of mica substrates after immersion in a 1 wt.% silica colloidal solution at pH 9 with added 0.1 M KNO_3 for different incubation times of a) 5 min, b) 10 min, and c) 1 h and then rinsing with an electrolyte solution containing the same content in KNO_3 salt at the same pH 9. Note that the mica surface gets rapidly covered by a single layer of silica nanoparticles as the incubation time gets longer.

peak surface roughness is about the spot size). Note that the particles appear slightly bigger than they are really because the image is a convolution between the geometry of the tip and the particle itself. As both sizes are comparable (≈20nm of radius at the apex of the tip and particles of ≈14nm diameter) the figure of convolution deforms the shape of a particle. The height profile indicates the adsorbed film is comprised of nanoparticles packed in a *single* layer, as the substrate underneath is clearly visible in the areas where no adsorption has occurred. The reason why the adsorption does not go beyond a single monolayer is quite trivial. As it will be shown in the following section two adsorbed silica layers are not mutually adhesive at this pH and they even repel free particles in bulk. Although particles are kinetically allowed to approach and contact the external colloidal/aqueous solution interface of the already adsorbed particles in the layer time to time, they are bounced back to the bulk since they cannot attach. Hence, monolayer is the final state of adsorption.

The force-distance profile between two silica monolayers coated-mica is comprised of *two distinct regimes*. At large separations, the interaction is dominated by an electrical double layer repulsion. At short separations the compression of the adsorbed silica layers on the mica surfaces induces a steep repulsion (steric wall, displacement of loosely bound particles) that may not be reversible upon decompression (adhesive silica layers). Both the long-range interaction and the adhesion at contact are dependent on solution conditions.

Long-Range Interaction

The force-distance profile is reversible upon compression or separation, as long as the surfaces do not come to contact (i.e.

for surface separations larger than *ca.* 30 nm). The eventual irreversibility due to some local disruption of the contact area when the two adsorbed layers get interpenetrated or are adhesive is addressed in the next section.

At large separations, the interaction is repulsive decaying exponentially with a decay-length $\kappa^{-1} = 1.4$ nm close to the Debye screening length expected at the ionic strength of the 1:1 electrolyte solution. It is attributed to the overlap of the electrical double layers originating from the charged silica-coated mica/aqueous solutions interfaces. In this distance regime the curves can be fitted using a numerical solution of the non-linearized Poisson-Boltzmann equation. At this stage the analysis discards the attractive contribution of the dispersion forces (negligible at large separations) and assumes some effective surface potentials, Ψ_S, the values of which will be discussed later. As the screening length, κ^{-1}, is determined by the solution condition, the fitting parameter Ψ_S governs alone the exponential repulsion at large separations. Actually the magnitude of Ψ_S is connected with the assumption made for the location of the diffuse layer onset. Another choice for the location of this plane will affect concomitantly the magnitude of the effective surface potential extracted from the fit to the same experimental data. A full discussion can be found, for example, in the analysis of the electrical double layer structure for smooth surfaces adsorbing hydrated ions.[48] Additional complications arise in the case of rough interfaces as it is impossible to strictly ascribe a location for the plane of origin of the double layer forces. Although small scale roughness effects are essentially smoothed for surfaces interacting with long range repulsive forces, the overall repulsion is reduced.[49] In the present case, the silica adsorbed layers are smooth at the nanometer scale only. For each coated mica it was assumed that the electrical diffuse layer originates at the plane of closest approach (i.e. at 14.5 nm, half the onset of the steric repulsion). This is an obvious simplification of the real electrical double layer structure as the analysis is based on the assumption that the onset of the diffuse double layer is not effected by the surface morphology of the silica/aqueous interface, while it is known that its hydrated structure is complex with eventual hairy (or gel-like) surface layer consisting of polysilicic acid chains protruding from the surface into the solution.[46,50–52]

The magnitude of the effective surface potential extracted from the force-distance profiles by comparison with such a calculation is −90 mV at pH 9. As a matter of fact, the fitting procedure only yields the absolute value of the surface potential. However, its negative sign was inferred by independent zeta potential measurements using the electrokinetic sonic effect (a technique particularly suitable for dispersions of nanocolloids where the generation of sound waves by an applied electric field can be used to determine the zeta potential; full details will be reported in a forthcoming article). The values obtained by the two different methods are in good agreement. The absence of discrepancy indicates that the coated film behaves as if its inner interface does not affect the long-range interaction. A full explanation would require an exact description of the grain region between the mica sheet and the adsorbed silica particles. This is beyond the scope of this work and as to simplify one may assume that globally this region is neutral electrically. Charge neutrality is ensured by the presence of ions in the grain boundary region and colloidal silica adsorb on the mica substrate by sharing their respective hydrated layers together with the hydrated shells of the ions. This picture is in good agreement with the pioneering studies of Matijevic and collaborators for explaining heterocoagulation.[53] The implications are two fold: (i) the simplifying assumptions over the choice of the origin of the diffuse layer are reasonable and do not affect Ψ_S to great extent. This being granted, the effective surface potential extracted from the fit can be identified with the potential at the boundary of the diffuse layer. It is the

signature of the silica/aqueous interface *only*. In other words the underlying mica substrate does not contribute to the electrostatic potential taken by the silica film; only the outer part of the silica film establishes the surface charge at the water interface and governs the ion distribution in the diffuse layer of the aqueous solution. Force measurements and colloidal stability can thus be compared; (ii) there is no charge reversal of the silica-coated mica substrate at this pH (and over the full pH range studied; see forthcoming article). This shows that in the presence of added nitrate potassium salt the negatively charged silica nanoparticles were able to adsorb on a mica substrate, that is also negatively charged in this electrolyte solution according to our previous study.[48]

Adhesion at Contact

When the two surfaces are approached the electrical double layer repulsion becomes dominated at short separations (< 30 nm) by a steric repulsion due to the compression of the adsorbed silica layers on mica. At pH 9, these layers are not adhesive as reversible force profiles were measured on approach and on separation (see Figure 2) and good reproducibility was obtained for subsequent runs (provided that not too large loads are applied as they can induce some rolling of the particles aside or some surface deformation). The observation of non adhesive behavior at basic pH is in agreement with the colloidal stability of bulk silica dispersion.[46,54–56] Note that our measurements are also in agreement with the anomalous colloidal behavior of silica sols where they are found to flocculate in medium pH, but are surprisingly stable around the isoelectric point (pH $\approx$ 2).[46,54–56] Indeed, a pull-off force was required to wrench the two surfaces apart for pH spanning *only* the range 4–6 (data not shown; will be reported in a forthcoming article), also in agreement with our previous measurements carried out on another colloidal silica type.[40]

Maintaining the native colloidal surface chemistry of the aqueous interface, our method shows the importance of surface chemistry in dictating interactions and introduces further applications of direct force measurement techniques to a wide range of colloidal systems of practical and industrial interest.

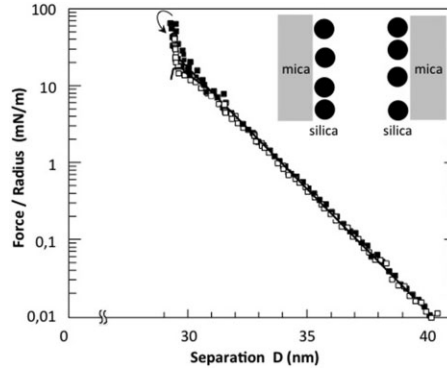

Figure 2.
Force F (normalized by the mean radius of curvature, R, of the surfaces) measured as a function of the surface separation, D, between two crossed mica cylinders that were left immersed for 3 h in a 1 wt.% silica solution of nanoparticles in the presence of added 0.1 M KNO_3 at pH 9.05 ± 0.05 and then rinsed with the same electrolyte solution. Solid symbols correspond to the force on approaching the surfaces, while the open symbols are the data measured upon separation. The overlap of the electrical double layers gives an exponential repulsion at large separations (decay length $\kappa^{-1} = 1.4$ nm corresponding to the expected Debye screening length at the ionic strength of the solution), while the compression of the two opposing coated silica layers gives a non adhesive (at this pH) steric repulsion from 29–30 nm, that is from about twice the size of a silica nanoparticle. Solid lines show D.L.V.O. calculation as the sum of the repulsive double-layer force, obtained by numerical solutions of the nonlinear Poisson-Boltzmann equation with constant surface potential (lower curve) or constant charge surface (upper curve) boundary condition, and the attractive van der Waals force calculated[48] in a triple layer model (silica-coated mica immersed in an electrolyte solution) using the Lifshitz theory (this gives an effective non retarded Hamaker constant of about 0.7×10^{-20} J) The diffuse layer boundary is supposed to be located at the onset of the hard wall ($D = 29$nm). Parameters for the double-layer force best-fit are: Debye length $\kappa^{-1} = 1.4$ nm, and surface potential at infinite separation $\Psi_S = -90$ mV).

Coating via Solvent Flow

Polyelectrolyte multilayers deposition on mica sheets is carried out following the procedure described previously.[41,42] We present here the procedure used for obtaining homogeneous films with a thickness growing linearly with the number of deposited polyelectrolyte layers. Similarly to these linearly growing films, one can obtain exponentially growing films as already reported in a previous article.[41] In short, after thickness calibration of the mica sheets glued silvered back onto the curved silica disks (radius ≈ 2 cm) of the Surface Force Apparatus, the surfaces are transferred from the apparatus into a sealed flow chamber to construct, *in situ*, the polyelectrolyte multilayer on the mica surfaces. Solutions of alternately positively PAH and negatively PSS charged polyelectrolytes are run through. The first deposited layer is the cationic polyallylamine (PAH), since mica is negatively charged in aqueous solution.[48] To insure homogeneous coated films, four or five (PAH/PSS) bilayers were deposited onto each mica surface in MES-tris buffer at pH 7.4. The method, described in details elsewhere,[42] yields homogeneous coverage of the mica surface, as demonstrated by AFM, and film homogeneity. It also avoids the rigidity influence of the supporting substrate on the elastic/plastic response of the polyelectrolyte multilayers upon applied loads when only two or fewer bilayers are deposited.[57,58] After several rinses in buffer, the coated mica surfaces with the polyelectrolyte multilayers are mounted back in the SFA chamber for force measurements. The operation is carried out under aqueous solution in order to prevent any drying of the surfaces. The films were studied at the same ionic strength used during their buildup and were never dried: this preserves the native structural organization of the polyelectrolytes multilayers which could otherwise collapse in the usual drying and washing process.

The force-distance profile between symmetric surfaces (each mica is coated with a $(PAH/PSS)_5$ film where 5 stands for the number of deposited layer pairs) is repulsive increasing steadily as the separation between the coated mica surfaces is reduced. Between 200 and 70 nm, the interaction is, in first approximation, exponentially repulsive. This is best seen in the semi-logarithmic plot of the force versus the separation distance of Figure 3. An electrical double-layer interaction cannot be attributed to the origin of the repulsion for several reasons. First, the measured decay-lengths lie in the 30–40 nm range, more than an order of magnitude larger than the Debye screening length expected at the ionic strength of the electrolyte solution. Secondly, reversible force profiles are not observed upon compression and on separation (see below). The origin of this repulsive regime observed both for linearly and exponentially growing films[41,42] is still on debate: one may invoke a steric hindrance or alternatively an increase of the osmotic pressure of the monomer and/or the counter-ions present in the film. When the films are further compressed, one reaches a transition zone starting roughly at separations of the order of 60 nm and ending at 30 nm with the occurrence of a steeper repulsive wall. This wall is the likely signature of a state where the multilayers are fully compressed.

One can expect that the threshold separation at which the repulsive interaction sets in (about 230 nm) corresponds to the distance where the films begin to interpenetrate. However, this separation distance is much larger than the 50–60 nm expected for two juxtaposed single $(PAH/PSS)_5$ films as measured by optical techniques under similar ionic strength conditions.[32] Conversely, the thickness value of 30 nm for the "solid" like core of the multilayers appears twice smaller than these predicted 50–60 nm thicknesses. Such differences, also observed by Blomberg *et al.*,[58] clearly indicates that the homogeneous monolayer model characterized by one refractive index and one film thickness does not correctly describe a multilayer that is rather characterized by a refractive index profile that extends from the core of the film into the solution.[32]

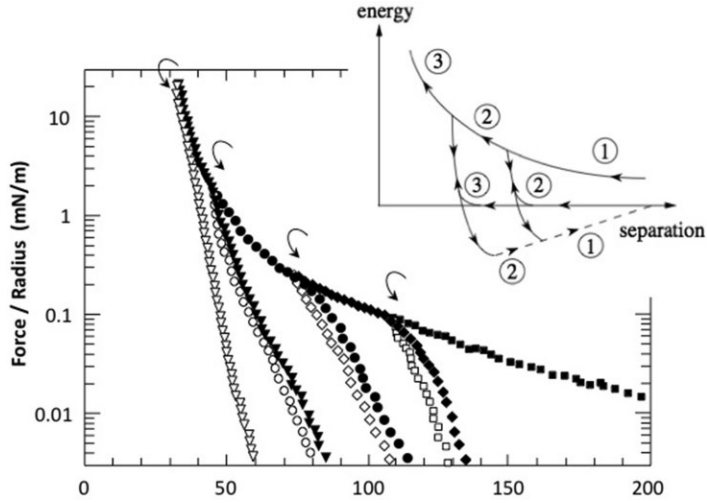

Figure 3.
Effect on subsequent approaches on the normalized force-distance profile for the $(PAH/PSS)_5$ linearly growing film system coating each mica surface. Upon compression (solid symbols), the local structure of the coated films is irreversibly affected, as indicated by both the hysteresis observed upon separation (empty symbols) and the changes in the magnitude and range upon subsequent approaches. The direction of the surface displacement was reversed at different separations. Note that upon a subsequent approach the force profile follows the path of the force measured on the preceding unload of the surfaces. Squares correspond to the first load-unload cycle, diamonds to the second cycle, circles to the third cycle and triangles to the fourth cycle. A schematic representation of the force-separation curves during consecutive load-unload cycles is given in the insert. The numbers 1–3 next to the profiles represent the cycle number. The dashed lines indicate that the surface jumps upon separation.

In order to gain insight into the dynamic behavior of the multilayers, subsequent approach/separation cycles are performed on the same contact area. A similar study was reported in detail in a previous article for asymmetric surfaces.[42] It was then stated that except for the attractive contribution at very large separations observed only in the case of oppositely charged multilayers,[42] the repulsive interaction is almost similar once the two opposite mica-coated films get interpenetrated. Therefore only a summary of the results are recalled here (see insert Figure 3 for a schematic). The force profile does not follow a reversible path when the direction of the surface displacement is reversed. Much larger compliances are observed upon the unload than upon loading and a slight adhesive force arises during the retraction. (Note that the term "high compliance" is used here in a context to describe a high stiffness and has no intention to refer to a high compliant, i.e. soft, system). The adhesive forces, whose strength increases as the two interpenetrating opposing films are compressed further, can have two origins: the disentanglements of the polyelectrolyte chains of the two interacting multilayers as well as the electrostatic interactions of PSS chains from one multilayer with PAH chains of the other film and *vice versa*. The adhesive forces are, however, rather small (between 0.002 and 0.3 mJ/m^2) indicating that the interactions between the chains of different multilayers must be rather small and limited. Note that the local structure of the multilayers is irreversibly affected once interpenetrated: upon a second reload, the starting point of the repulsive regime is about the separation at which the initial unload has left the surfaces free of interaction. This is the separation at which the polyelectrolyte chains had disentangled from the films that were interpenetrated upon the first compression. Remarkably,

the films interact by following the same upwards path upon reloading as followed previously downwards upon the unload (Figure 3). Steep compliance is maintained as the separation is decreased down to the former turning point. If the direction of the surface displacement is reversed once more at that turning point the same path will be followed again upon the new unload. Conversely, if the turning point is passed upon further reduction of the surface separation, the steep compliance is abandoned there, and the force-distance profile catches up with the original decay-length of the exponential repulsion as if no unload/load cycle had taken place in between. The same features take place whatever the separation distance at which the turning point is positioned. Note that similar behaviors are reproducibly observed if the unload/load cycles are carried out at a new virgin spot area.

As discussed previously[42] our results suggest two remarks: (1) linearly growing films of polyelectrolyte multilayers, such as PAH/PSS, behave as glassy materials in agreement with the suggestion made by Cohen Stuart and coworkers[59] and (2) the disruption that occurs during the unload path affects only the outer part of the film. The entanglements and the interactions of the polyelectrolyte chains of the two films must thus only concern the two outer layers of the films. This is consistent with the small rupture forces that are measured. The structural modifications induced by a primary compression over a given range are irreversible and the film relaxation observed during the separation cycles must only affect each part of the film very locally, most of the film remains in a frozen state. This again shows that the polyelectrolyte chains in the (PAH/PSS) multilayers do not rearrange over large distances and explains why these films keep a periodic structure after deposition and give rise to Bragg peaks in neutron reflectivity experiments.[60] The glassy state of these systems is also supported by the fact that all the systems described here retain their features over a week-long period. The absence of differences in the force profiles as the films are stored, not only qualitatively but also in terms of magnitude and range, indicates that the native structure of the multilayers do not evolve significantly over this period of time. Also, once disrupted, the films do not evolve over time: even long annealing times (days) do not allow the film to recover the initial situation. This indicates that the local structure of the multilayers adsorbed on both mica surfaces is irreversibly affected once interpenetrated. Furthermore, the measured adhesion, which also remains unchanged over a week-long period, does not present a dependence on the resting time at contact under an applied load (up to a few hours) nor on the number of cycles (load-unload) previously performed at the same contact position. This additional observation supports the conclusion that polyelectrolyte chains do not undergo significant rearrangement or diffusion within the PAH/PSS multilayers once the film structure is built or disrupted.

The implications of our force measurements provide a route to tune the internal structure of polyelectrolyte multilayers to obtain films and/or shells with desired properties such as biocompatibility, stability, density, morphology, together with a control of the mechanical properties of the films at the nanometer scale. This is of particular interest for enhancing the adhesion of the coating to the biological cells[61] and for engineering nanocapsules and nanocarriers whose the shell is biocompatible and/or biodegradable in order to deliver drugs to the target site.[62] The two experimental procedures, that we have just presented (this section § 3-2 and the previous one § 3-1), can be indeed combined to investigate these two aspects. Thus, we have studied core/shell nanoparticles synthetized by Schneider and Decher.[63] These gold nanoparticles (AuNPs) are ensheated with five bilayers of PAH and PSS by alternate coating to yield core/shell nanoparticles with a general structure AuNP/$(PAH/PSS)_5$ and an outer diameter about 23 nm; nanosized template-free capsules can be obtained as the result

of gold core dissolution of the template core/shell nanoparticles by cyanide etching.[63] Thanks to our experimental procedures that maintain the structural features and do not alter the physicochemical surface properties, we can provide the conditions to be fulfilled for having robust nanocapsules that are able to form stable aqueous colloidal dispersions.[64]

Coating by Langmuir-Blodgett Deposition

As for the other two experimental procedures, the solid support consists of thin, molecularly smooth, back-silvered mica sheets, glued onto fused silica hemicylinders with an average radius of curvature $R \approx 2$ cm. We have followed the pioneering work of Marra and collaborators for preparing SFA surfaces homogeneously covered by phospholipids monolayers and/or bilayers by Langmuir-Blodgett deposition.[13–15] After thickness calibration of the mica sheets in air, the silica disks are transferred into a Langmuir trough (installed in a clean room of class 10000) to add the assembly of the bilayers by Langmuir-Blodgett deposition. The NIMA trough as well as the two computer controlled barriers are made of Teflon. It possesses a maximum surface area of 300 cm^2 (10cmx30cm), a minimum surface area of 50 cm^2, and is filled with approximately 250 ml water subphase. The ultra pure Millipore water (18.2 MΩ cm^{-1}) is degased for 30 min under vacuum beforehand to reduce the possibility of small bubbles being trapped in the deposited layers. The trough, placed on an antivibration table, is covered by a Plexiglas hood to insure good thermal and mechanical stability. The compounds are dissolved in chloroform-methanol (see § 2-1), and the solution is spread on the free water surface with a Hamilton syringe, typically using spread volumes between 40 and 60 μL. The surface pressure Π is measured by the Wilhelmy plate method using a filter paper, defined as $\Pi = \gamma_0 - \gamma$ where γ_0 is the surface tension of the pure subphase and γ is the surface tension in the presence of amphiphiles at the interface. After 30 min or 1 h of equilibration of the monolayer in order to let the chloroform and methanol to evaporate, the compression is started with a compression speed of 10 cm^2/min and isotherms are recorded at a temperature of 25 °C.

As already stated mica is the most suitable substrate for SFA, being hydrophilic, atomically smooth and with an exchangeable surface charge density of one charge per 0.48 nm^2. All samples are prepared with a first layer of DSPE built atop a mica surface, deposited at 40 mN/m, by lifting up the holder supporting the mica sheet hemicylinder out of the water trough at a 5 mm/min speed. Phospholipids with the zwitterionic phosphoethanolamine (PE) headgroups bind electrostatically to the negatively charged mica surface. At their highest packing density, the PE headgroups and their two chains have a surface area of 0.43 nm^2 closely matching the surface lattice and charge of mica.[13] They provide a particularly smooth hydrophobic surface for deposition of a second monolayer.[13–15,22,23,27,28,65] With a transfer ratio close to one, an hydrophobic layer of DSPE is thus deposited onto the mica substrate with an excellent homogeneous surface coverage and practically no defects over the whole area (≈ 1 cm^2) as checked by independent Atomic Force Microscopy imaging. This procedure is repeated for the second mica sheet holder.

To deposit the outer hydrophilic layer of the ultimate bilayer the DSPE-coated mica mounted on its holder is dipped from top through the water interface on which was previously spread a solution of the desired material (Figure 4). Thus, for the results presented below (see Figures 5 and 6), the second deposited layer on one holder is a mixture of DPPC with the cholesteryl β-CDs whereas for the other holder it is a mixture of DPPC with the STLs. The second layer is always deposited at 30 mN/m with a deposition speed set to 2 mm/min. The transfer ratios have been observed to be larger than 0.9 for the second layer.

Then the holders are transferred back to the SFA chamber under degassed ultra

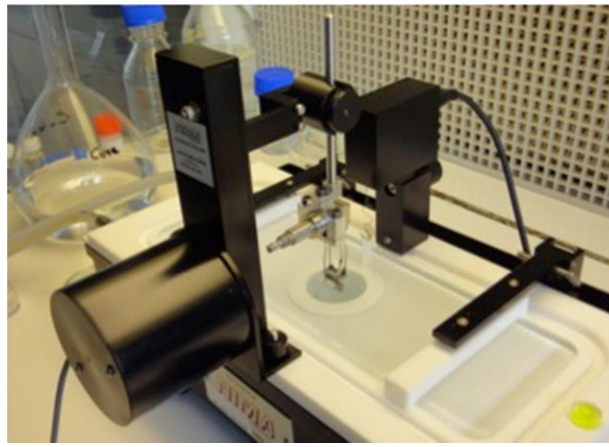

Figure 4.
View of the current Langmuir-Blodgett deposition process where a second layer is deposited on the DSPE hydrophobic monolayer coated-mica surface by progressively immersing its holder onto which it is attached (one can recognize the hemicylinder disk mounted on the double cantilever spring of the SFA device) into the water subphase of the Langmuir trough. For photo convenience the Plexiglas hood ensheating the trough for thermal stability has been removed and the Teflon barriers have been opened.

pure water. This prevents the surfaces of experiencing any environment outside their native structural organization by avoiding any drying and collapse of the second hydrophilic layer.

By the deposition procedure described above, two sets of experimental configurations have been sought in order to measure the force-distance profiles as a function of the separation between the two deposited bilayers:

- the *symmetric* configurations with bilayers made of the same material; for instance a bilayer of DSPE/DPPC interacting in water with a like bilayer DSPE/DPPC.
- the *asymmetric* configurations where on one mica surface is deposited a bilayer of a certain type (for example DSPE/DPPC), while on the other mica is deposited a bilayer of different chemical nature (for example DSPE/DPPC-β-CD).

In this study all the experimental combinations have been realized, both in symmetric configuration (DPPC vs. DPPC; DPPC-STL vs. DPPC-STL; DPPC-β-CD vs. DPPC-β-CD) and in asymmetric configuration (DPPC vs. DPPC-STL; DPPC vs. DPPC-β-CD; DPPC-β-CD vs. DPPC-STL). It was observed that, *only* this latter configuration, contrary to the 5 other configurations (data not shown), yields to a peculiar adhesive behavior, which is the signature of a specific interaction between the STL chains capped with the adamantane ligands and the β-CD receptors. Similar observations were observed for the key-lock interaction between streptavidin and biotin,[22,23] the specific interaction between nucleotides,[24] and the tethered ligand-receptor bond formation.[27,28]

More precisely it is observed that all configurations present a certain number of common features in the measured *repulsive* regimes. At large separations, the interaction is exponentially repulsive as the separation between the bilayers is reduced, and reversible upon approaching or separating the surfaces. An electrical double-layer best fit (Figure 5) indicates that the effective surface potential seen at infinite separation is about 44 mV. This low value is in good agreement with the interaction potential inferred from recent X-ray scattering experiments on phospholipids

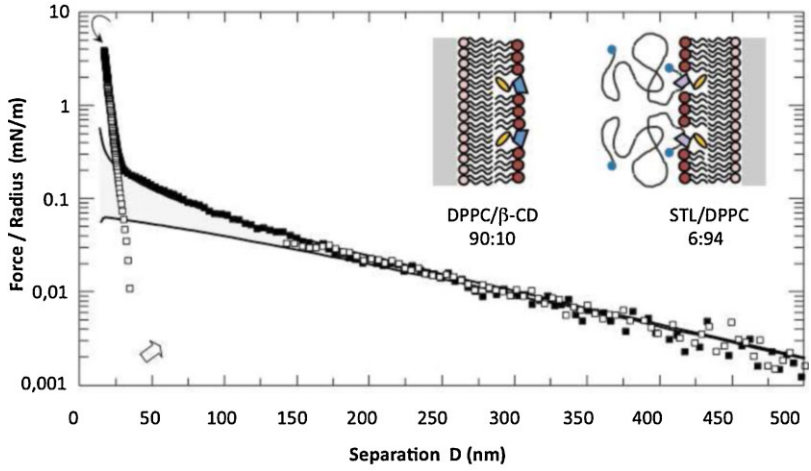

Figure 5.
Measured forces, *F*, normalized by the mean radius of curvature *R* of the surfaces between crossed mica cylinders coated with phospholipid bilayers modified with STLs (in the ratio DPPC/STL 94:6) and cholesteryl β-CD receptors (DPPC/β-CD 90:10), as a function of the separation, *D*. Solid symbols correspond to the normalized force on approaching the surfaces in water while the open symbols are the data measured upon separation. Solid lines are the best-fit numerical solution to the nonlinear Poisson-Boltzmann equation with constant surface charge (upper curve) or constant surface potential (lower curve) boundary conditions. The D.L.V.O. curves presented here are obtained with an effective non-retarded Hamaker constant of 1×10^{-20} J and the assumption that the outer Helmholtz plane coincides with the onset of the steric wall. Parameters for the double-layer force best fit indicate that the effective surface potential seen at infinite separation is $\Psi_s \sim 44$ mV and that the coated surfaces interact through a large Debye screening-length ($\kappa^{-1} = 110$ nm) as expected for charged surfaces immersed in pure water in equilibrium with CO_2. For surface separations smaller than ~30 nm the force-distance profile deviates from the pure electrical double layer repulsion due to the compression of the STL brush. Then at smaller separations, a steeper compliance of the repulsion is experienced due to the steric contact between the two opposite bilayers (~10 nm). In this small separations range the force-distance profile becomes irreversible and eventually adhesive as a pull-off force must be applied to wrench the surfaces apart (empty symbols; arrow).

bilayers.[66] It indicates the presence of a small amount of surface charges (~0.001 e/nm^2), necessarily present owing to the amphoteric character of the phosphatidylcholine group. Thus, in this distance regime the bilayers interact through an electrical double layer repulsion resulting from the weak surface charges of the phospholipids. At very short separations, the encountered strong compliance is generated by the steric interaction of the two bilayers in contact. Only the configurations in the presence of STL brush show an additional repulsion on top of the exponential electrical double layer repulsion at the intermediate separation range: this additional repulsion is due to the brush compression (Figure 5).

The main difference between the 6 configurations shows up essentially in the *non reversibility* of the force-distance profile when the direction of the surface displacement is reversed (at short separations), which generates an *adhesive behavior* eventually. This is only observed in the asymmetric configuration where the STL's adamantane caps are interacting with opposite β-CD receptors. To gain insight into the sliding tethered ligand behavior, subsequent approach/separation cycles are performed on the same contact area. The direction of the surface displacement is reversed at different separations during the approach of the two opposite films (Figure 6).

As already mentioned, one observes full reversibility of the force-distance profile upon approach or separation of the surfaces as long as they remain beyond the extent of

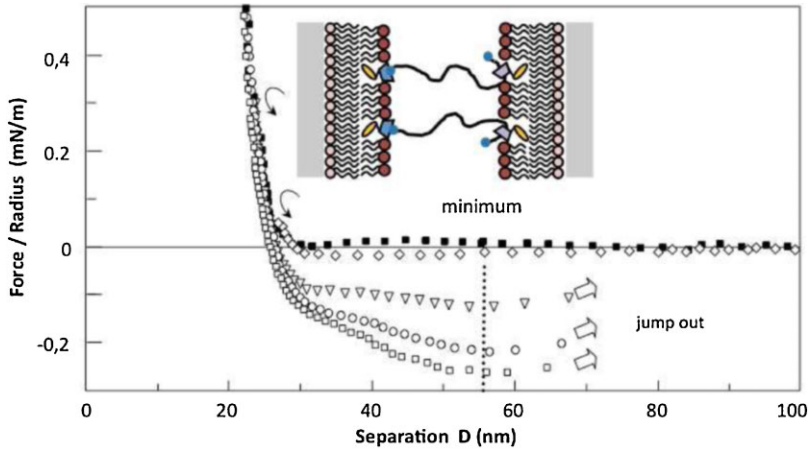

Figure 6.
Effect on subsequent load/unload cycles on the normalized force-distance profile after subtraction of the electrical double layer and van der Waals interactions (as calculated by the D.L.V.O. fit at constant surface charge boundary condition) from the total measured forces of Fig. 5. The remaining interaction is the contribution of the sliding tethered ligand chains interacting with the opposite β-CD receptors. As all the forces on approach of the surfaces are similar, only one set of data is reported (solid squares). Conversely, the forces measured on withdrawal of the surfaces (all other empty symbols) depend on the turning point separation (indicated by curved arrows) where the surface displacement is reversed. The smaller turning point separation the larger adhesion is, and the two surfaces jump apart due to the mechanical instability of the cantilever (arrows). Remarkably the minimum of the attractive profile occurs at about the same location $D \approx 55$ nm indicating that the ligand-receptor bonds can be broken only if the STL chains are sufficiently elongated by acquiring enough stretched energy.

the polymer brush. Conversely, below this threshold separation the force profile no longer follows a reversible path when the surface direction of the surface displacement is reversed. Larger compliances are observed upon the unload than upon loading and a slight adhesive force arises during the retraction. The strength of this adhesive force due to ligand – receptor bond formation increases for compression/separation cycles with increasingly smaller turning points in separation (Figure 6) and eventually the two surfaces jump apart due to the mechanical instability of the cantilever. Remarkably, the minimum of the attractive profile occurs at about the same location $D \approx 55$ nm, which is far away from the steric wall. This indicates that the ligand-receptor bonds can be broken only if the STL chains are sufficiently elongated by acquiring enough stretched energy. Subsequent reload sequences give similar results. Furthermore, the observed attractive behavior does not present a dependence on the resting time at contact under a given applied load (up to a few hours) nor on the number of cycles (load-unload) previously performed at the same contact position. This latter feature suggests that the bilayers deposited by LB do not exchange material when they get into mechanical contact: receptors are not pulled out of the membrane and the binding sites remain intact after bond breakage.

Our results show that the force profiles upon withdrawal are typical for tethered ligand-receptor interactions. Due to the polymer tether, the range of the initially short ranged specific adamantane-CD interaction is extended by the length of the fully extended chain. Sliding Tethered Ligands (STLs) based on topological complexes between polyethylene glycols (PEG) and cholesteryl α-cyclodextrins (CDs), which can be inserted into phospholipid membranes due to their cholesteryl anchor, provide a design to extend the interaction range between two opposing surfaces up to

tens of nanometers while keeping specific molecular recognition through ligand-receptor pairs specific adhesion.

Conclusion

Three main experimental procedures have been proposed to overcome the difficulties often encountered in surface preparation for direct force measurements. Through examples we have shown how intricate surface chemistry and complex structural organization of real systems can be preserved or mimicked. Our methods of preparing the macroscopic surfaces used in the SFA can be shown to be easily generalized to any real system, as the structural organization of the thin coated film, the native surface chemistry and the physicochemical surface properties of the interface are maintained. Furthermore, as each of the SFA surfaces can be prepared independently, not only symmetric configurations of two like interacting surfaces can be realized, but also asymmetric configurations can be realized in a controlled way to directly measure the interactions between two unlike surfaces. The play with different surface configurations allows the experimentalist to investigate the mechanical stability of thin films, the colloidal stability of nanoparticles dispersions, the heterocoagulation occurring between charged surfaces, the origin of adhesion at contact, the ligand-receptor specific interaction, etc. Our method introduces further applications of direct force measurement techniques to a wide range of systems of practical and industrial interest, such as the development of advanced materials, of nanocarriers for targeted drug delivery, of versatile bio-adhesive substrates that can better accommodate surface roughness and dynamic fluctuations, etc.

Acknowledgments: Martin Bauer, Natalia Bushmarina, Agi Kulcsar, and Jalal Machou are gratefully acknowledged for their contribution in the surface preparations and Jean Iss for technical help in the SFA measurements. The Sliding Tethered Ligand project has been supported by the French Research Program ANR-07-NANO-016-02.

[1] J. N. Israelachvili, "*Intermolecular and Surface Forces*", Academic Press, London **1995**.
[2] P. Kékicheff, in: "*Electrostatic Effects in Soft Matter and Biophysics*", C. Holm, P. Kékicheff, R. Podgornik, Eds., Kluwer Academic Publishers, Dordrecht, The Netherlands **2001**, vol. *46*, p. 205.
[3] B. V. Derjaguin, I. I. Abrikosova, E. M. Lifshitz, *Quart. Rev.* **1956**, *10*, 295.
[4] L. Knapschinsky, W. Katz, B. Ehmke, H. Sonntag, *Colloid Polym. Sci.* **1982**, *260*, 1153.
[5] D. Tabor, R. H. S. Winterton, *Nature* **1968**, *219*, 1120.
[6] J. N. Israelachvili, G. E. Adams, *J. Chem. Soc. Faraday Trans. I* **1978**, *74*, 975.
[7] G. Binning, C. Quate, Ch. Gerber, *Phys. Rev. Lett.* **1986**, *56*, 930.
[8] W. A. Ducker, T. J. Senden, R. M. Pashley, *Nature* **1991**, *353*, 239.
[9] E. Finot, E. Lesniewska, J.-C. Mutin, J.-P. Goudonnet, *Langmuir* **2000**, *16*, 4237.
[10] P. M. McGuiggan, J. N. Israelachvili, *Chem. Phys. Lett.* **1988**, *149*, 469.
[11] P. Richetti, L. Moreau, P. Barois, P. Kékicheff, *Phys. Rev. E* **1996**, *54*, 1749.
[12] R. G. Horn, *Biochim. Biophys. Acta* **1984**, *778*, 224.
[13] J. Marra, *J. Colloid Interface Sci.* **1985**, *107*, 446.
[14] J. Marra, J. N. Israelachvili, *Biochemistry* **1985**, *24*, 4608.
[15] J. Marra, *Biophys. J.* **1986**, *50*, 815.
[16] D. Leckband, J. N. Israelachvili, *Quart. Rev. Biophysics* **2001**, *34*, 105.
[17] T. Afshar-Rad, A. I. Bailey, P. F. Luckham, W. MacNaughtan, D. Chapman, *Colloids Surf.* **1988**, *31*, 125.
[18] P. Kékicheff, B. W. Ninham, *Europhys. Lett.* **1990**, *12*, 471.
[19] P. Kékicheff, W. A. Ducker, B. W. Ninham, M.-P. Pileni, *Langmuir* **1990**, *6*, 1704.
[20] M. Malmsten, P. Claesson, G. Siegel, *Langmuir* **1994**, *10*, 1274.
[21] T. Nylander, P. Kékicheff, B. W. Ninham, *J. Colloid Interface Sci.* **1994**, *164*, 136.
[22] C. A. Helm, W. Knoll, J. N. Israelachvili, *Proc. Natl. Acad. Sci. U. S. A.* **1991**, *88*, 8169.
[23] D. E. Leckband, J. N. Israelachvili, F. J. Schmitt, W. Knoll, *Science* **1992**, *255*, 1419.
[24] F. Pincet, E. Perez, G. Bryant, L. Lebeau, C. Mioskowski, *Phys. Rev. Lett.* **1994**, *73*, 2780.
[25] D. Leckband, *Nature* **1995**, *376*, 617.
[26] S. Sivasankar, W. Brieher, N. Lavrik, B. Gumbiner, D. Leckband, *Proc. Natl. Acad. Sci. USA* **1999**, *96*, 11820.
[27] J. Y. Wong, T. L. Kuhl, J. N. Israelachvili, N. Mullah, S. Zalipsky, *Science* **1997**, *275*, 820.

[28] C. Jeppesen, J. Y. Wong, T. L. Kuhl, J. N. Israelachvili, N. Mullah, S. Zalipsky, C. Marques, *Science* **2001**, *293*, 465.
[29] R. G. Horn, J. N. Israelachvili, J. Marra, V. A. Parsegian, R. P. Rand, *Biophys. J.* **1988**, *54*, 1185.
[30] P. Kékicheff, H. K. Christenson, *Phys. Rev. Lett.* **1989**, *63*, 2823.
[31] P. Richetti, P. Kékicheff, P. Barois, *J. Phys. II France* **1995**, *5*, 1129.
[32] G. Ladam, P. Schaad, J.-C. Voegel, P. Schaaf, G. Decher, F. Cuisinier, *Langmuir* **2000**, *16*, 1249.
[33] M. Bauer, T. Charitat, C. Fajolles, G. Fragneto, J. Daillant, *Soft Matter.* **2012**, *8*, 942.
[34] M. Bauer, M. Bernhardt, T. Charitat, P. Kékicheff, C. Fajolles, G. Fragneto, C. Marques, J. Daillant, *Soft Matter.* **2013**, *9*, 1700.
[35] P. Kékicheff, *et al.*, *to be submitted.*
[36] J. N. Israelachvili, *J. Colloid Interface Sci.* **1973**, *44*, 259.
[37] B. V. Derjaguin, *Kolloid Z.* **1934**, *69*, 155.
[38] E. Blomberg, P. M. Claesson, H. K. Christenson, *J. Colloid Interface Sci.* **1990**, *138*, 291.
[39] O. Spalla, P. Kékicheff, *J. Colloid Interface Sci.* **1997**, *192*, 43.
[40] D. Atkins, P. Kékicheff, O. Spalla, *J. Colloid Interface Sci.* **1997**, *188*, 234.
[41] A. Kulcsar, P. Lavalle, J.-C. Voegel, P. Schaaf, P. Kékicheff, *Langmuir* **2004**, *20*, 282.
[42] A. Kulcsar, J.-C. Voegel, P. Schaaf, P. Kékicheff, *Langmuir* **2005**, *21*, 1166.
[43] D. C. Prieve, E. Ruckenstein, *J. Colloid Interface Sci.* **1977**, *60*, 337.
[44] M. A. V. Axelos, D. Tchoubar, R. Jullien, *J. Physique France* **1986**, *47*.
[45] C. A. Johnson, A. M. Lenhoff, *J. Colloid Interface Sci.* **1996**, *179*, 587.
[46] R. K. Iler, "*The Chemistry of Silica*", Wiley-Interscience, New York **1979**.
[47] B. Dahneke, *J. Colloid Interface Sci.* **1975**, *50*, 89.
[48] V. E. Shubin, P. Kékicheff, *J. Colloid Interface Sci.* **1993**, *155*, 108.
[49] G. Cevc, S. Svetina, B. Zeks, *J. Phys. Chem.* **1981**, *85*, 1762.
[50] J. A. Kitchener, *Faraday Discuss.* **1971**, *59*, 379.
[51] T. Hiemstra, W. H. Riemsdijk, *Colloids Surf.* **1991**, *59*, 7.
[52] M. Kobayashi, F. Juillerat, P. Galletto, P. Bowen, M. Borkovec, *Langmuir* **2005**, *21*, 5761.
[53] H. Kihira, E. Matijevic, *Langmuir* **1992**, *8*, 2855.
[54] L. H. Allen, E. Matijevic, *J. Colloid Interface Sci.* **1969**, *31*, 287.
[55] L. H. Allen, E. Matijevic, *J. Colloid Interface Sci.* **1970**, *33*, 420.
[56] J. Depasse, A. Watillon, *J. Colloid Interface Sci.* **1970**, *33*, 431.
[57] K. Lowack, C. A. Helm, *Macromolecules* **1998**, *31*, 823.
[58] E. Blomberg, E. Poptoshev, P. M. Claesson, F. Caruso, *Langmuir* **2004**, *20*, 5432.
[59] D. Kovacevic, S. van der Burgh, A. de Keizer, M. A. Cohen Stuart, *J. Phys. Chem. B* **2003**, *107*, 7998.
[60] M. Lösche, J. Schmitt, G. Decher, W. G. Bouwman, K. Kjaer, *Macromolecules* **1998**, *31*, 8893.
[61] L. Richert, F. Boulmedais, P. Lavalle, J. Mutterer, E. Ferreux, G. Decher, P. Schaaf, J.-C. Voegel, C. Picart, *Biomacromolecules* **2004**, *5*, 284.
[62] J. Kreuter, "*Colloidal Drug Delivery Systems*", Marcel Dekker, New York **1994**, vol. *66*, 353.
[63] G. Schneider, G. Decher, *Nano Letters* **2004**, *4*, 1833.
[64] P. Kékicheff, G. Schneider, G. Decher, *submitted.*
[65] T. L. Kuhl, D. E. Leckband, D. D. Lasic, J. N. Israelachvili, *Biophys. J.* **1994**, *66*, 1479.
[66] A. Hemmerle, L. Malaquin, T. Charitat, S. Lecuyer, G. Fragneto, J. Daillant, *Proc. Natl. Acad. Sci. USA* **2012**, *109*, 19938.

